Fresenius J Anal Chem (2001) 371 : 934–938
DOI 10.1007/s002160101041

ORIGINAL PAPER

Viktor Kanický · Vítězslav Otruba · Jean-Michel Mermet

Calibration graphs for Ti, Ta and Nb in sintered tungsten carbide by infrared laser ablation inductively coupled plasma atomic emission spectrometry

Received: 2 April 2001 / Revised: 28 June 2001 / Accepted: 10 July 2001 / Published online: 17 October 2001

Abstract Infrared laser ablation (IR–LA) has been studied as a sample introduction technique for the analysis of sintered cobalt-cemented tungsten carbide materials by inductively coupled plasma atomic emission spectrometry (ICP–AES). Fractionation of cobalt was observed. Linearity of calibration plots was verified at least up to 15% Ti, 8% Ta, and 3% Nb. Above 1% (m/m) Ti, Ta, and Nb, the repeatability of results was better than 3% R.S.D. The relative uncertainty at the centroid of the calibration line was in the range from ±3% to ±4% for Ti, Ta, and Nb with internal standardization by tungsten and up to ±5% without internal standardization. The limits of detection were 0.004% Ti, 0.001% Ta, and 0.004% Nb. Elimination of the cemented hardmetal dissolution procedure is the main advantage of this method.

Introduction

In twenty years laser ablation inductively coupled plasma atomic emission spectrometry (LA–ICP–AES) has become an efficient tool for direct elemental analysis of solids. The importance of LA sampling increases when complex and time-consuming decomposition procedures are needed for sample dissolution, because a laser beam enables vaporization of chemically resistant materials. Dissolution of advanced ceramics requires combined fusion and acid decomposition [1, 2]. These high-tech construction materials are widely used in many load-bearing applications, e.g. cutting tools, car-engine components, heat exchangers, turbines, wear parts, and aerospace [3].

Tungsten carbide (WC) is one of the most frequently used materials. This extremely hard and resistant material is used in the form of plasma-sprayed coatings or sintered pieces. The determination of Co in cobalt-cemented WC coatings by means of LA–ICP–AES has been studied with both ultraviolet (LA) and infrared (IR) lasers [4, 5]. Linear calibration for Co was obtained for UV laser ablation using internal standardization by tungsten [4], whereas for IR laser ablation internal standardization was not necessary and selective vaporization was not observed in a wide range of irradiance [5]. The aim of this work is to evaluate the possibility of application of IR–LA–ICP–AES to the analysis of cobalt-cemented tungsten carbide hardmetal samples.

Experimental

Instrumentation

LA–ICP–AES was performed with a Lina-Spark laser and an Optima 3000 DV ICP spectrometer. The Lina-Spark atomizer (W. Vogel, LSA, Switzerland) is based on a Q-switched Nd:YAG laser (model Surelite I/20; Continuum, USA) operated at a wavelength of 1064 nm with a pulse duration of 7 ns. The maximum attainable pulse energy (200 mJ), adjusted by setting the Xe-flashlamp discharge voltage, was applied with a rate of repetition of 20 Hz. In the Lina-Spark device, the target surface is located at a fixed position and the sample-to-lens distance can be adjusted by changing the lens position. Throughout this work the laser beam was focused 16 mm behind the target surface, using a lens with a 158-mm focal length at the wavelength of 1064 nm The diameter of ablation craters was 1.1 mm and the calculated irradiance was 3.2 GW cm^{-2}. This irradiance value has been found optimum for the determination of Co in cobalt-cemented tungsten carbide coatings [5], determination of trace elements in agricultural soil samples [6], and in steel analysis [7].

The ablation can usually be performed either at a fixed spot or during sample displacement (translation, rotation) in the plane of the beam incidence. The Lina Spark instrument offers the possibility of rotational motion. With this system the ablated area can be enlarged by moving the laser beam over two superimposed circles, which differ in diameters and circular speeds. The eccentric circular trajectory of the laser beam is performed by means of the motion of the motor-driven focusing lens. A 2 mm-circle trajectory at a speed of 1 mm s^{-1} was used in some experiments. For analytical measurements fixed-spot ablation was used. The carrier gas pro-

V. Kanický (✉) · V. Otruba
Laboratory of Plasma Sources for Chemical Analysis –
Laboratory of Atomic Spectrochemistry,
Faculty of Science, Masaryk University Brno,
Kotlářská 2, 61137 Brno, Czech Republic
e-mail: viktork@chemi.muni.cz

J.-M. Mermet
Laboratoire des Sciences Analytiques, Bât. 308,
Université Claude Bernard-Lyon I, 69622 Villeurbanne, France

Table 1 Comparison, linear regression analysis[a], of analytical results from XRF and from solution analysis with ICP–AES

Analyte	n	r	b	s_b	t_b	a	s_a	t_a	t_{crit}
Ti	13	0.9993	1.0260	0.01220	2.1311	0.144	0.071	2.0217	2.201
Ta	16	0.9997	0.9869	0.00650	2.0154	0.0353	0.0231	1.5294	2.145
Nb	16	0.9997	0.9873	0.00647	1.9629	–0.00726	–0.00918	0.7916	2.145

[a] Number of samples n; correlation coefficient r; slope b of the regression line of XRF against ICP; standard deviation of the slope s_b; calculated value t_b of the Student test of the slope b against 1; intercept a of the regression line of XRF vs. ICP; standard deviation of the intercept s_a; calculated value t_a of the Student test of the intercept a against zero; critical values of the Student test t_{crit} for n-2 degrees of freedom and at the level of significance α=0.05

vided and controlled by the ICP instrument is introduced into the 14-mL ablation chamber of the Lina-Spark. The ablated material is transported along polyamide tubing (length 1.5 m, i.d. 4 mm) into the ICP. Each ablation sampling was performed for 100–220 s and the steady-state part of the signal was used for analytical evaluation.

A Perkin–Elmer Optima 3000 ICP DV was used in lateral observation mode at the optimized viewing height of 12 mm. The 40-MHz ICP was operated at a forward power of 1.0 kW; the outer, intermediate, and Ar carrier gas flow rates were 15.0, 0.5, and 0.7 L min^{-1}, respectively. The polychromator with an echelle grating is provided with segmented-array charge-coupled device detectors (SCD). The spectral bandwidth per pixel is 0.006–0.010 nm in the range used – 207–337 nm. The sum of three adjacent pixels of the SCD was used to measure the gross emission intensity (peak-area mode). This total intensity was corrected for the off-peak background emission. Only background-corrected signals are used throughout this work. With a sampling time of 1 s and integration times of 10–100 ms, a signal reading was available every three seconds.

Samples

Sintered Co-cemented tungsten carbide samples were obtained from the hardmetal products manufactured by a powder metallurgy plant – Pramet Tools, Šumperk, Czech Republic, a subsidiary company of Seco Tools, Sweden. The composition of block samples (12×15×5 mm^3) was within the ranges (% m/m): W 52–82, C 4.6–8, Co 3–25, Ti 0.02–15, Ta 0.16–8.5, Nb 0.07–3.4, and V 0.2–0.3. Samples were routinely analyzed after decomposition – by ICP–AES at Pramet and by XRF spectrometry in the Research Institute of Inorganic Chemistry (VÚAnCh), Ústí n. Labem, Czech Republic.

XRF analysis was performed with the PW 1404 sequential spectrometer (Philips, The Netherlands) equipped with a rhodium target X-ray tube and the LiF 220, Ge 111, and TlAP analyzer crystals. Percentages were calculated by means of Uniquant software (Philips), a pre-calibrated analytical program for semiquantitative analysis of unknown samples. Uniquant determines the net intensities of fluorescence lines and corrects for matrix interelement effects using α-coefficients computed by use of the method of fundamental parameters. The samples were embedded in poly(methyl methacrylate) in the shape of 40-mm disks. This form was useful for both the XRF analysis and the LA–ICP spectrometry.

The ICP solution analyses and XRF results were compared by use of linear regression analysis (Table 1). Slopes of linear regression lines (correlation of XRF results with those from ICP) were tested by use of the Student test against unity and intercepts were tested against zero. Calculated t-values were less than critical values for the corresponding degrees of freedom at the level of significance α=0.05. Consequently neither constant nor proportional systematic error is apparent from correlation of results from XRF and ICP analysis.

Results and discussion

Selection of analytical lines

Analytical lines were selected on the basis of investigation of spectral interferences with the Ti, Ta, and Nb lines in the presence of W and Co matrices. The mutual spectral interferences of W, Ti, Ta, and Nb were also taken into consideration. Interferences were examined by using pneumatic nebulization of solutions. The spectral lines studied were: Ti II 334.941 nm, Ti II 336.121 nm, Ti II 337.280 nm; Ta II 226.230 nm, Ta II 233.198 nm, Ta II 240.064 nm; Nb II 269.706 nm, Nb II 292.781 nm, and Nb II 309.418 nm. The resulting optimum lines/background correction positions used for laser ablation experiments were: Ti II 337.280 nm/–0.020 nm; Ta II 240.064 nm/+0.028 nm; Nb II 309.418 nm/–0.099 nm; W II 207.911 nm/–0.030 nm.

Optimization of ablation conditions

The dependence of signal intensities and corresponding R.S.D. values on laser beam irradiance were studied for Ti, Ta, and Nb lines by focusing in the range from 18 to 12 mm behind the target surface, i.e. within the material. The starting point of these experiments was the optimization of the Lina Spark instrument described in detail elsewhere [5]. Samples were ablated at a constant (maximum) energy of 200 mJ and a repetition rate of 20 Hz. Fixed-spot ablation and ablation with circular motion were used. Finally, focusing 16 mm behind the surface and fixed spot ablation were used for the development of an analytical method. The diameter of ablation craters was 1.1 mm and the calculated irradiance was 3.2 GW cm^{-2}. Chosen ablation conditions correspond with those which have been found optimum for the determination of Co in cobalt-cemented tungsten carbide coatings [5], determination of trace elements in agricultural soils [6], and analysis of polymers [7] and steels [7, 8].

Signals as a function of time

Ablation signals as a function of time differ for fixed-spot ablation and ablation during circular motion. For circular ablation a steady-state signal is not reached even after 130 s

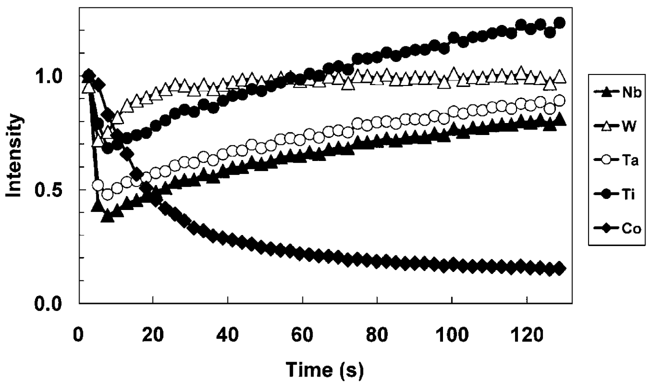

Fig. 1 Circular motion ablation signals; circle diameter 2 mm at a speed of 1 mm s^{-1}, laser pulse energy 200 mJ, laser repetition rate 20 Hz, focusing 16 mm behind the sample surface; sample composition (% m/m): 6.3 C, 6.0 Co, 3.62 Ti, 3.82 Ta, 1.50 Nb; analytical lines: Ti II 337.280 nm, Ta II 240.064 nm, Nb II 309.418 nm, W II 207.911 nm, and Co II 228.616 nm

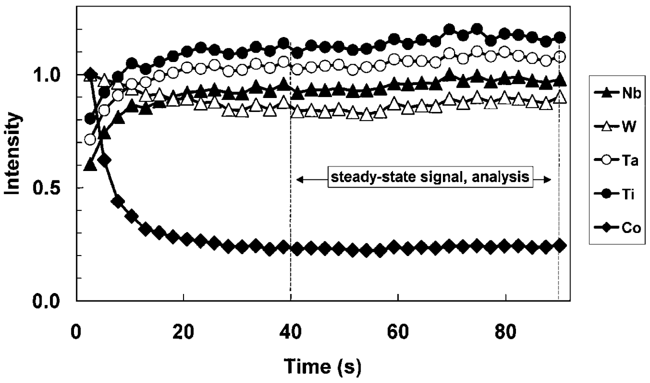

Fig. 2 Fixed-spot ablation signals; laser pulse energy 200 mJ, laser repetition rate 20 Hz, focusing 16 mm behind the sample surface; sample composition (% m/m): 6.3 C, 6.0 Co, 3.62 Ti, 3.82 Ta, 1.50 Nb; analytical lines: Ti II 337.280 nm, Ta II 240.064 nm, Nb II 309.418 nm, W II 207.911 nm, and Co II 228.616 nm; the plateau indicated was used for R.S.D. calculation and analysis

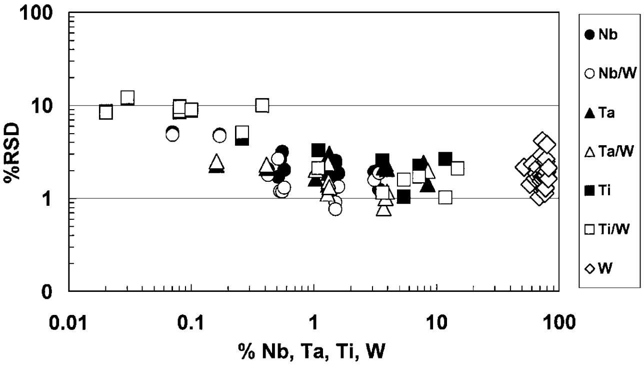

Fig. 3 Relative standard deviation (%) of the fixed-spot ablation signal calculated on the basis of 20 replicates in the signal plateau defined in Fig. 2

(Fig. 1), whereas for fixed-spot ablation a plateau is reached after 40 s (Fig. 2). The polishing of the hardmetal sample surface before routine LA–ICP analysis would require an extra device, and, therefore, the sample surface was intentionally left unpolished for our ablation experiments. According to reported experience with the Lina Spark [5, 6, 7, 8], a sufficient pre-ablation period always yields steady-state signals. Generally, time evolution of signals is caused by different physical and/or chemical states of a surface in comparison with in-depth properties of the sample material [9, 10]. In contrast with time-correlated signals of trace elements in soils [6] and constituents in steel [7], however, some differences between elements arise in sintered carbides. Identical time dependence is observed for titanium, tantalum, and niobium line intensities whereas the cobalt line intensity significantly decreases, and the tungsten line intensity is similar to those of Ti, Ta, and Nb (Figs 1 and 2). This is probably because Ti, Ta, Nb, and W are used in the form of carbides, whereas Co is added as metal in the technology of powder metallurgy production. It seems that fractionation probably occurs during both fixed-spot and circular ablation. Fixed-spot ablation was adopted for development of the analytical method to keep the pre-ablation time reasonably short. The average of emission intensity readings (20 replicates) over the steady-state period (40–90 s) is taken as the analytical signal (Fig. 2).

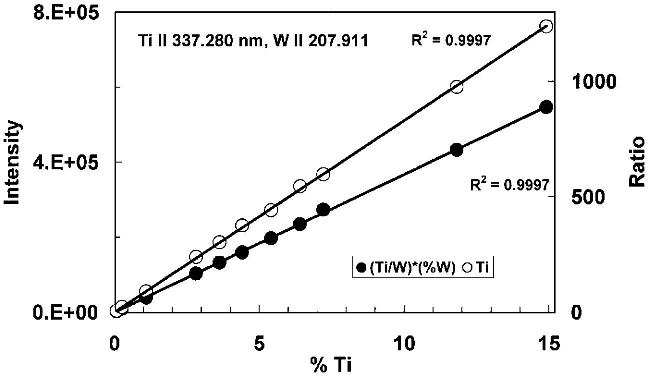

Fig. 4 Calibration line for Ti II 337.280 nm line, without and with internal standardization by use of W II 207.911 nm

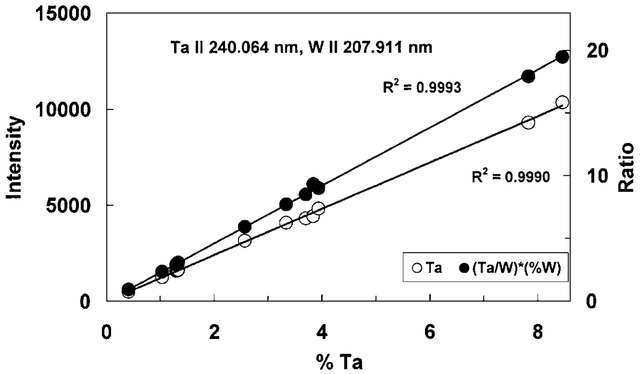

Fig. 5 Calibration line for Ta II 240.064 nm line, without and with internal standardization by use of W II 207.911 nm

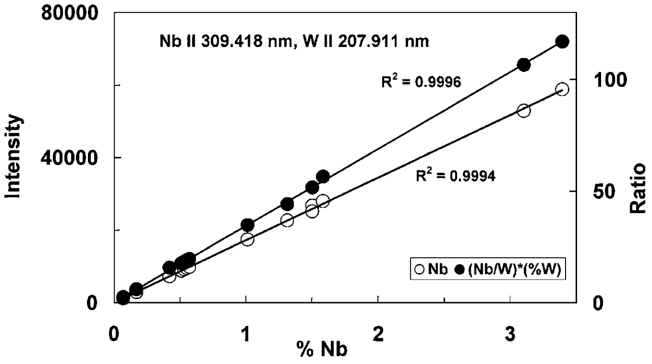

Fig. 6 Calibration line for Nb II 309.418 nm line, without and with internal standardization by use of W II 207.911 nm

Precision of the analytical signal, limits of detection

The relative standard deviation (R.S.D., %) of the fixed-spot ablation signal was calculated on the basis of 20 replicates in the signal plateau defined in Fig. 2. the dependence of this R.S.D.% on the amounts (%) of Ti, Ta, Nb, and W are log–log plotted in Fig. 3. In the range 52–82% W in studied samples, the R.S.D.% of the tungsten signal is constant and equal to 2.0%. The R.S.D. is <3% for amounts of Ti, Ta and Nb above 1% in the samples. Internal standardization by use of tungsten does not affect the R.S.D. values significantly. With increasing concentration of the elements, c, the R.S.D.% decreases approximately according to the function $k/\sqrt[3]{c}$ where k is a constant for a certain element. Limits of detection (0.004% Ti, 0.001% Ta and 0.004% Nb) were calculated by extrapolating this dependence to R.S.D.=47%, which is the value corresponding to the 3σ-definition of limit of detection and the single point background correction.

Calibration, repeatability of results, analysis of real samples

Calibration plots were constructed for Ti, Ta, and Nb under optimum conditions described in the experimental section. The ablation was repeated three times at different locations on each sample – i.e. the number of replicates, p, was equal to 3 at each percentage level. The number of calibration samples, m, was equal to 11 for Ti, 13 for Ta, and 14 for Nb. Calibration curves were fitted using a computer program WinStat [11] which also tests the linearity by the F-test (lack-of-fit test) [12] and automatically selects the calibration model (linear, quadratic). The linear calibration graphs are presented in Figs. 4 5 6 for Ti, Ta, and Nb, respectively. Relative widths of confidence intervals about the centroid [13] are reduced by internal standardization by use of the W II 207 nm line, as follows from Table 2.

The repeatability R.S.D. [14, 15] was calculated on the basis of six analyses at the different locations on a real tungsten carbide sample, no. 1060U10. The repeatability

Table 2 Characteristics of calibration lines

Spectral line		λ (nm)	Uncertainty of centroid (% rel.) Internal standard		Centroid (% m/m)	Calibration range (% m/m)	Number of calibration samples and replicates
			Yes	No			
Ti	II	337.280	3.73	5.05	5.27	0.08–14.90	11; 3
Ta	II	240.064	2.31	2.62	3.10	0.41–8.45	13; 3
Nb	II	309.418	2.81	3.51	1.16	0.07–3.39	14; 3

Table 3 Analysis of tungsten carbide real sample 1060U10 and statistical testing of differences between LA–ICP–AES results and pneumatic nebulization (PN) ICP–AES results

		Ti	Ta	Nb
PN–ICP–AES	c (%, m/m)[a]	3.62	3.83	1.50
	s_r (%, m/m)[b]	0.08	0.10	0.04
LA–ICP–AES without internal standard	c (%, m/m)[a]	3.65	3.79	1.47
	s_r (%, m/m)[b]	0.10	0.10	0.06
	F-test[c]	1.46	1.02	1.80
	t-test[d]	0.42	0.50	0.74
LA–ICP–AES with internal standard (W II 207.9 nm)	c (%, m/m)[a]	3.64	3.78	1.52
	s_r (%, m/m)[b]	0.07	0.07	0.03
	F-test[c]	2.27	1.73	3.20
	t-test[d]	0.31	0.67	0.58

[a] arithmetic mean, number of replicates: 3 for PN-ICP–AES, 6 for LA–ICP–AES

[b] repeatability standard deviation [15]

[c] F-testing of standard deviations of LA–ICP–AES vs. PN-ICP–AES, F_{crit} (5;2)=19.296

[d] Student test of the difference between means, t_{crit}(0.05; 7)=2.365

R.S.D.% obtained with a sample containing 3.62% Ti, 3.83% Ta, and 1.5% Nb was 2.7%, 2.5% and 3.9%, respectively. When tungsten is used as internal standard the repeatability R.S.D.% is improved and reaches the values 1.8%, 1.9%, and 2.2% for Ti, Ta, and Nb, respectively.

Tungsten carbide real sample no. 1060U10 was analyzed by the developed laser ablation ICP–AES method and the results of Ti, Ta, and Nb determination were compared with those obtained by ICP–AES analysis of solutions. Triplicate analysis (including decomposition) was performed with solutions, whereas ablation was repeated six times at different locations on the sample. The statistical significance of differences between the mean values was tested by use of the Student test. The results presented in Table 3 imply there is no statistically significant difference between the results from solution-based ICP analysis and those from the laser ablation ICP technique.

Conclusions

The possibility of direct determination of Ti, Ta, and Nb in sintered cobalt-cemented tungsten carbides has been proved by use of infrared laser ablation in combination with ICP–AES. The precision of the results is comparable with those of a solution-based ICP–AES method. No systematic error was found between analytical results obtained using the solution-based ICP method and those from LA–ICP–AES. Elimination of the decomposition of the cemented hardmetal is the main advantage of this method. During ablation the behavior of the cobalt line signal with increasing time was, however, different from that for titanium, tantalum, niobium, and tungsten; this will be the object of further study.

Acknowledgements V.K. and V.O. gratefully acknowledge the Grant Agency of the Czech Republic for bestowing the research grant GACR 203/00/0415. The authors wish to thank Perkin–Elmer for the loan of the Optima 3000 DV ICP spectrometer and W. Vogel (LSA, Sarl, Cully, Switzerland) for construction of the Lina-Spark Atomizer.

References

1. Farinas JC, Barba MF (1992) J Anal At Spectrom 7:869–875
2. Farinas JC, Barba MF (1992) J Anal At Spectrom 7:877–882
3. Schwartz MM (1992) (ed) Handbook of structural ceramics. McGraw–Hill, New York
4. Kanický V, Otruba V, Mermet JM (2000) Spectrochim Acta B 55:575–586
5. Kanický V, Otruba V, Mermet JM (2000) Spectrochim Acta B 55:1601–1610
6. Musil P, Otruba V, Kanický V, Mermet JM (2000) Spectrochim Acta B 55:1747–1758
7. Hemmerlin M, Somas D, Dubuisson C, Loisy F, Poussel M, Mermet JM (2000) Fresenius J Anal Chem 368:31–36
8. Kanický V, Otruba V, Novotný K, Musil P, Mermet JM (2001) Fresenius J Anal Chem 370:387–392
9. Chan WT, Russo RE (1991) Spectrochim Acta B 46:1471–1486
10. Mao X, Chan WT, Russo RE (1997) Appl Spectrosc 51:1047–1053
11. Mestek O (1997) WinStat, QM-Service Ltd, Prague
12. Massart DL, Vandeginste BGM, Deming SN, Michotte Y, Kaufman L (1988) Chemometrics, a textbook. Elsevier, Amsterdam
13. Mermet JM (1994) Spectrochim Acta B 49:1313–1324
14. IUPAC (1998) Compendium of analytical nomenclature, definitive rules 1997. Blackwell Science
15. Eurachem Working Group (1998) The fitness for purpose of analytical methods, a laboratory guide to method validation and related topics. LGC, Teddington